EurJIC European Journal of Inorganic Chemistry
ChemPubSoc Europe
FULL PAPER

DOI:10.1002/ejic.201402587

Synthesis of Atomically Precise Silver Clusters by Using the Miscibility Principle

Atanu Ghosh[a] and Thalappil Pradeep*[a]

Keywords: Cluster compounds / Phase diagrams / Silver / S ligands / Solvent effects

A new strategy to synthesize a diverse array of organic-soluble, atomically precise silver clusters has been developed. The technique is based on the miscibility principle of solvents and uses no phase-transfer agents; various clusters of masses 8.0, 13.4, 22.8, 29.2, and 34.4 kDa were synthesized by changing the reactant composition. We have also synthesized the well-known $Au_{25}(SR)_{18}$ cluster by the same method. Among the silver clusters formed, we have studied the new 13.4 kDa species, which has unique steplike features in its UV/Vis spectrum, in detail by mass spectrometry and other analytical techniques. The compound has been assigned as $Ag_{68}(SR)_{34}$, which is reported for the first time. By time-dependent studies, we have shown that the synthetic route follows the bottom-up approach. The material forms microcrystals. We hope that the proposed synthetic strategy will extend the area of atomically precise clusters.

Introduction

Among the emerging categories of nanosystems are the atomically precise clusters of noble metals protected with monolayers, which are referred to as quantum clusters (QCs), nanomolecules, clusters, or super atoms. The interesting structural, optical, and electronic properties of QCs[1] as well as their potential applications in catalysis,[2] biomedicine,[3] and nanoelectronics[4] have made these systems important for chemistry and materials science as a whole. The systematic size evolution of these clusters to bulk materials allows the investigation of the emergence of size-dependent properties.

Although the two-phase method for the synthesis of noble metal nanoparticles has been highly effective,[5] the materials synthesized by this route contain the phase-transfer agent (PTR, discussed in the Supporting Information), which is a persistent impurity in detailed analysis owing to the interdigitation of monolayers.[6] Although methods that avoid PTRs exist, they have not produced a large variety of materials, especially for silver, and the materials are most often polydisperse.[7] The solubility of the nanosystems formed in the organic phase and the requirement of reducing agents in the aqueous phase lead to reduction at the interface, and the products formed phase-separate naturally. However, a careful control of the composition of a three-component system can also lead to phase separation, which can be conveniently used for reduction, cluster growth, and isolation of products without the use of a PTR. A three-component system that exhibits two well-defined phases can be converted to one phase by the precise control of the phase compositions. This control can result in the transfer of solutes from one phase to the other. In that process, a chemical reaction may occur, and the products can be separated without the use of additional chemicals. For atomically precise clusters of noble metals, the most rapidly expanding family of noble metal nanosystems, water is an essential ingredient of the reaction as most of the reduction is performed by $NaBH_4$ or its variants.[5b,7b,8] The transfer of metal ions into a suitable organic solvent or mixture and reduction by the nascent hydrogen liberated in a homogeneous phase can eventually lead to clusters, which phase-separate at the newly formed phase boundary. This phase transfer can be controlled with suitable pairs of solvents and, thus, the use of a PTR can be avoided completely. Here, we introduce this versatile strategy for the synthesis of an array of atomically precise clusters. Although several clusters are known, mostly of gold, new synthetic methodologies are required to realize many of the unknown clusters, especially those of silver.

Results and Discussion

The phase diagram of the three-component system used for the experiments is shown in Figure 1 (A). Multiple solvent compositions were used for cluster synthesis, as indicated in the phase diagram. As shown in the photographs (Figure 1, B), the syntheses yielded different clusters in each of these solvent compositions with the same quantities of reagents (more details of the procedure are provided in the Supporting Information). The MALDI MS and UV/Vis

[a] DST Unit of Nanoscience (DST UNS) and Thematic Unit of Excellence (TUE), Department of Chemistry, Indian Institute of Technology Madras
Chennai 600036, India
E-mail: pradeep@iitm.ac.in
http://www.dstuns.iitm.ac.in

Supporting information for this article is available on the WWW under http://dx.doi.org/10.1002/ejic.201402587.

© 0000 Wiley-VCH Verlag GmbH & Co. KGaA, Weinheim

spectra of the products formed (Figure S2) confirm the formation of different cluster cores. At each of the solvent compositions, different clusters can also be formed by varying the reactant ratios. In this communication, we introduce this method by describing one of the new clusters, namely, $Ag_{68}SBB_{34}$ (SBB = the thiolate form of BBSH, 4-*tert*-butylbenzyl mercaptan), in some detail. This corresponds to the solvent composition marked "d" in the phase diagram (Figure 1).

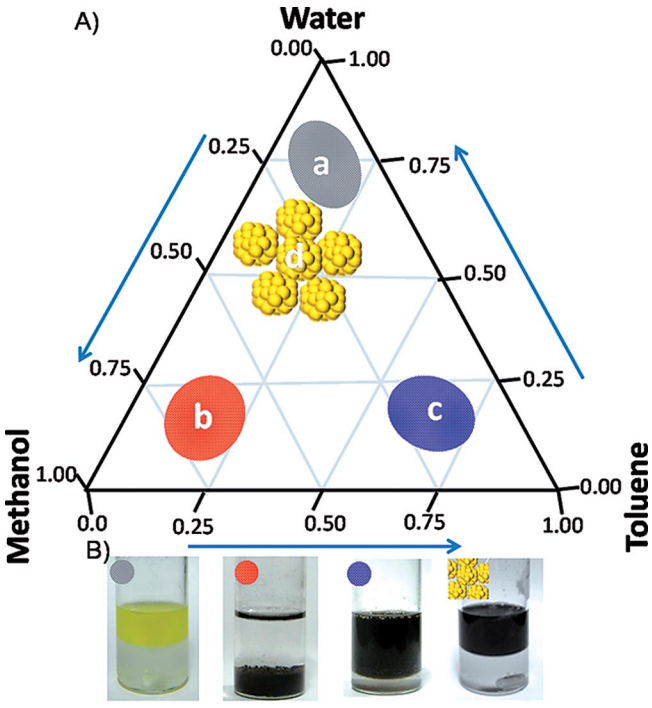

Figure 1. (A) Phase diagram of the three-component (water, methanol, and toluene) system in which the synthesis was performed. The four different regions in the phase diagram at which the reactions were performed are indicated. (B) Photographs of the reaction products. Different clusters were formed under each of these conditions.

The miscibility principle may be illustrated with a specific example close to region "d" in Figure 1 (A). Initially, methanol (3 mL) was used (Figure S3A), and toluene (3 mL) was added; this mixture formed a single phase as they are completely miscible (Figure S3B). Next, water (2 mL) was added to this homogeneous phase. As water is completely miscible with methanol and partly miscible with toluene, water/methanol formed a phase and separated from the toluene phase (Figure S3C). In Figure S3D, toluene is replaced by chloroform (3 mL). As the chloroform-rich phase is denser than water/methanol, the former moved to the bottom when water was added. To extend this phase separation to cluster synthesis, we performed the reduction of $Ag^{I}SBB$ thiolates in a three-component (water/toluene/methanol) system. Initially, $AgNO_3$ (20 mg, 0.12 mmol) was dissolved in methanol (3 mL). To this solution, toluene (3 mL) containing BBSH (132 μL, 0.72 mmol) was added; this resulted in a color change from colorless to turbid yellow-white owing to the formation of $Ag^{I}SBB$ thiolates (Figure 2, a_1). At this point, toluene and methanol are miscible, and the mixture appears as a uniform phase. The solution changes to brown upon the addition of ice cold water (2 mL) containing $NaBH_4$ (45 mg, 1.20 mmol) with constant stirring; the color change indicates the reduction of $Ag^{I}SBB$ (Figure 2, a_2). Upon standing for 10 min, the final result is the separation of two distinct phases. The bottom phase is a water/methanol mixture and is colorless, and the top dark brown portion contains the cluster in a toluene-rich phase (Figure 2, a_3). When we used chloroform instead of toluene, the bottom phase contained the cluster (Figure 2, a_4). The phase boundaries can be seen clearly owing to the extraction of the clusters into these phases. Nearly pure clusters were collected from the top layer in Figure 2 (a_3), whereas impurities such as thiolates and metal ions were collected in the bottom phase (Figure S4a). The only possible impurity along with cluster is excess thiol (Figure S4b). The clusters were precipitated by the addition of excess methanol, which also removes the thiol present in the sample. The precipitate was washed four to five times with methanol, and the cluster powder was obtained by rotary evaporation. The synthetic method is highly robust and can be reproduced easily. It does not strongly depend upon conditions such as temperature or the purity of the materials, unlike typical cluster syntheses. We performed the reaction during the prevailing summer (ca. 40 °C) and winter (ca. 25 °C) conditions in Chennai and also used normal and dry solvents. We confirmed the identity of the products by UV/Vis spectroscopy and matrix-assisted laser desorption

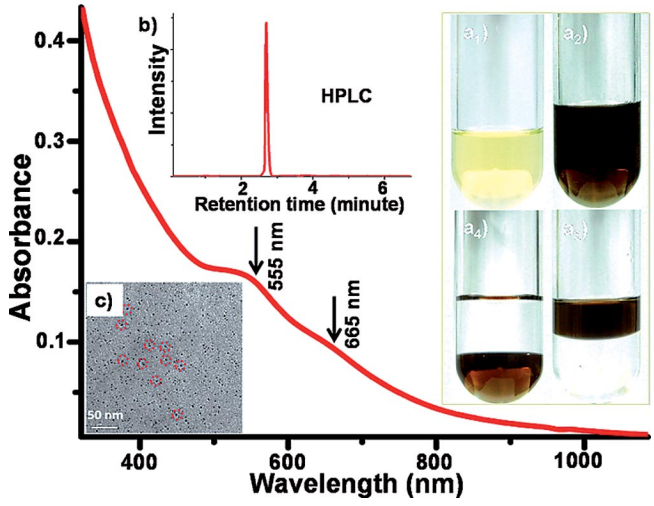

Figure 2. The UV/Vis spectrum of the as-synthesized cluster. The spectrum has steplike features, which are characteristic of small clusters. The arrows indicate the peak positions. (a) Photograph of the synthetic process: (a_1) Ag and thiol in methanol/toluene mixture (single phase), (a_2) after the addition of $NaBH_4$, (a_3) 10 min after stopping the reaction (two well-separated phases with the cluster at the top), and (a_4) separated phases with chloroform instead of toluene, the cluster is in the bottom phase. A magnetic pellet is at the bottom of each of the test tubes. (b) Single peak in the HPLC chromatogram of the crude product, which confirms the formation of a single cluster. (c) TEM image of the purified cluster. The approximate core size of the cluster is 1.2 nm. Some clusters are marked with circles.

 © 0000 Wiley-VCH Verlag GmbH & Co. KGaA, Weinheim

ionization mass spectrometry (MALDI MS). These data are discussed below. The purity is estimated to be ca. 95% on the basis of the MALDI MS data. Similar results were obtained by replacing toluene with $CHCl_3$. All of the results presented here are for the clusters obtained from the water/toluene/methanol system. In Figure S5, we have shown the importance of the solvent mixture. Larger quantities of the cluster were prepared by scaling up the synthesis (the details are in Supporting Information). The precipitate was washed with methanol and then dissolved in toluene for the various measurements.

The UV/Vis spectrum of the crude cluster in toluene is shown in Figure 2. Two well-defined steps are seen, as is observed for atomically precise clusters.[9] The purity of the sample is the most important issue in this type of synthesis. We have performed high-performance liquid chromatography (HPLC) of the sample with tetrahydrofuran/MeOH (THF/MeOH, 70:30) as the mobile phase (Figure 2, b) to check the purity of the sample. Only one peak was seen in the HPLC chromatogram, and the chromatographed sample has the same UV/Vis spectrum as that of the crude product (Figure 2). In this experiment, a C18 column (250 × 4.6 mm) was used with a flow rate of 1 mL/min under isocratic conditions (the details are in the Supporting Information). These results confirm the formation of a single cluster,[10] which was identified as $Ag_{68}SBB_{34}$ from studies presented below. The optical spectrum shows molecule-like transitions at 555 and 665 nm, unlike those of plasmonic nanoparticles. These peaks are redshifted in comparison with those of the analogous $Au_{68}SR_{34}$.[11] The TEM image of the cluster is shown in Figure 2 (c). The cluster core size is nearly 1.2 nm. In Figure S7, we have shown that the cluster is stable towards electron beam irradiation, unlike other atomically precise clusters such as Au_{18} and Au_{25}.[8,12]

Detailed mass analyses were conducted by MALDI MS and laser desorption ionization (LDI) MS to determine the composition of the cluster. For several of the monolayer-protected gold and silver clusters, the exact compositions were determined by MALDI MS.[10a,10c,11,13] The LDI MS and MALDI MS analyses show that the cluster is highly pure as no peaks other than those of interest were found. The MALDI MS of the sample was recorded with *trans*-2-[3-(4-tertbutylphenyl)-2-methyl-2-propenylidene]malononitrile (popularly known as DCTB) as the matrix. The cluster gave a single peak at m/z = 13.4 kDa in the MALDI MS spectrum (Figure 3). No other peaks were observed in a wide range from m/z = 15 to 100 kDa. It is important to point out that the spectrum was measured at the threshold laser power, which results in spectra with no or reduced fragmentation.[11]

We assigned the peak to a cluster of composition $Ag_{68}SBB_{34}$. To confirm this assignment, we have performed LDI MS studies of the sample. In MALDI MS measurements, we can obtain the true mass of the cluster. However, during the LDI MS measurements, the laser can cleave the C–S bonds upon ionization. Instead of Ag_mSBB_n, we can obtain the mass spectrum corresponding to the Ag_mS_n core,

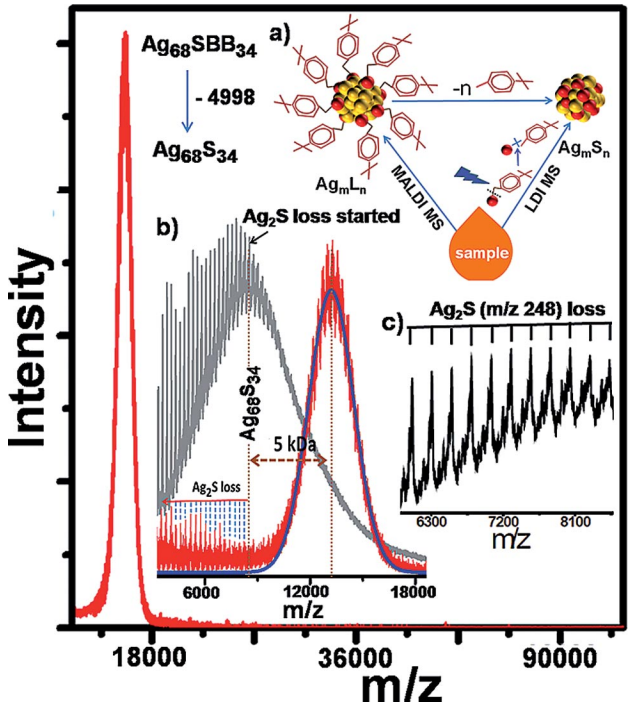

Figure 3. MALDI MS spectrum of the cluster, which shows a single peak at m/z = 13.4 kDa. (a) Representation of MALDI and LDI MS. The MALDI MS shows peaks of Ag_mL_n (L is Ligand), whereas LDI MS shows peaks of the Ag_mS_n core (LDI breaks the C–S bonds). (b) Expanded MALDI MS (red trace) and LDI MS (gray trace) spectra of the cluster. The red trace was fitted with a Gaussian function, which is shown in blue. The mass difference between the center of the Gaussian curve fitted for $Ag_{68}(SBB)_{34}$ cluster and the peak position from where Ag_2S loss started is 5 kDa. Inset: Ag_2S loss in the MALDI MS spectrum, which begins at ca. 8.4 kDa. This overlaps with the mass of the $Ag_{68}S_{34}$ core. (c) The formation of the Ag_mS_n core is confirmed by the successive loss of Ag_2S molecules (m/z = 248) in the LDI MS spectrum, shown as a series.

in addition to systematic fragmentations. The C–S bond cleavage can also happen during MALDI but it occurs at increased intensity only with higher laser powers. A representation of the observed MALDI and LDI processes is shown in Figure 3 (a). The MALDI MS and LDI MS spectra are compared in Figure S8 and show a mass difference of ca. 5 kDa. This mass loss supports the presence of 34 ligands on the cluster [147 × 34 = 4998; 147 is the mass of the ligand after C–S cleavage)]. The expanded Gaussian-fitted MALDI MS and LDI MS spectra for the cluster are shown in Figure 3 (b). The mass difference between the center of the $Ag_{68}(SBB)_{34}$ peak and the position from which Ag_2S loss started is 5 kDa. The highest mass at which Ag_2S loss is clearly seen in the MALDI MS spectrum is ca. 8.4 kDa, which corresponds to the $Ag_{68}S_{34}$ core. The formation of the Ag_mS_n core is further confirmed from the series of silver sulfide peaks spaced at m/z = 248, which are due to the fragmentation of the parent Ag_mS_n core (Figure 3, c).

The thermogravimetric (TG) analysis of $Ag_{68}(SBB)_{34}$ under a nitrogen atmosphere displayed a sharp mass loss of 44.8% in the 110–500 °C window (Figure S9). The observed

 © 0000 Wiley-VCH Verlag GmbH & Co. KGaA, Weinheim

mass loss matches the organic weight fraction (45.0%) expected for $Ag_{68}(SBB)_{34}$. The SEM images with elemental mapping and the energy-dispersive X-ray spectroscopy (EDAX) spectrum are shown in Figure S10. In SEM/EDAX, the Ag/S ratio seen was uniform throughout the sample and almost matched the calculated value for $Ag_{68}(SBB)_{34}$ (1:0.51). The absence of a sodium peak (remnant of the reducing agent) indicated that the sample is highly pure. The SEM image of the material after crystallization is shown in Figure S11. Although microcrystals were seen, they were not large enough for single-crystal studies. The ligation of BBSH in the form of thiolate (SBB) attached to the Ag core was confirmed by the absence of an S–H stretching peak at 2562 cm^{-1} in the Fourier transform infrared (FTIR) spectrum of the cluster (Figure S12). The existence of clusters was confirmed by the X-ray diffraction (XRD) pattern of the sample, which showed a broad peak centered at $2\theta \approx 38°$. The spectrum was compared with the characteristic face-centered cubic (fcc) diffractions exhibited by 15 nm diameter metallic Ag@H_2MSA (H_2MSA: mercaptosuccinic acid) nanoparticles (Figure S13).[14] Several silver clusters show only broad features.[7b,10d,15] A broad peak at $2\theta \approx 35°$ was also observed for gold clusters.[10e,16] The nature of the metal and monolayer binding were confirmed by X-ray photoelectron spectroscopy (XPS). The XPS survey spectrum of the as-synthesized cluster is shown in Figure S14A. Only the expected elements are present; therefore, this also shows that the sample is very pure. The Ag atoms are almost in the zero oxidation state (Figure S14B). The S $2p_{3/2}$ binding energy (BE) of 163.2 eV is characteristic of the thiolate ligand, which supports the IR data (Figure S14C). The BE is calibrated with respect to that of C 1s at 284.5 eV.

For any synthesis, it is always important to know the synthetic route. To gain some understanding of the synthesis process, we have performed time-dependent mass and UV/Vis analyses. Such UV/Vis spectra showed that the cluster formation is complete within 120 min (insets of Figure 4). A broad peak at 550 nm appeared initially at 15 min. A shoulder peak at 665 nm started to appear at 60 min and is more prominent at 120 min. The absence of further changes at 180 and 240 min (Figure S15) confirmed the conclusion of the reaction. The time-dependent MALDI MS spectrum after 15 min of reaction shows a single peak corresponding to 10.3 kDa for the cluster (Figure 4). At 60 min, the presence of a larger cluster at m/z = 11.5 kDa is seen. Finally, at 120 min, the sample shows a dominant peak at 13.4 kDa. As discussed earlier, in the LDI process, the C–S bond cleavage occurs, which will give information about the Ag_mS_n core. We also performed LDI for the 10.3, 11.5, and 13.4 kDa clusters to understand their core masses. As the reaction time increases, the core mass and mass loss increase, which implies that the number of silver atoms and ligands increase with time. In the LDI experiment, the formation of Ag_mS_n was confirmed by the observation of a series of silver sulfide peaks owing to the fragmentation of the parent Ag_mS_n core. This data supports that the cluster evolution follows a bottom-up approach. The yield of the Ag_{68} synthesis depends on the solvent (toluene or chloroform) used. For toluene, the yield was ca. 55%, whereas the yield was ca. 60–65% for chloroform.

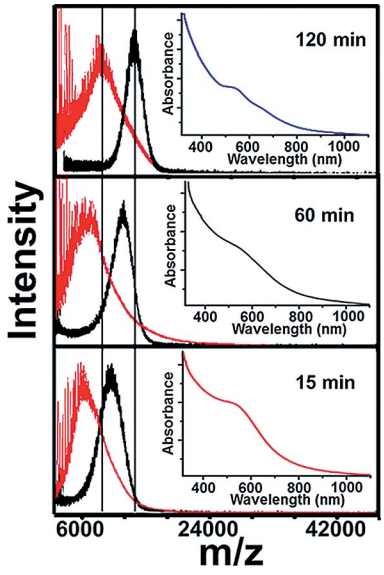

Figure 4. Time-dependent mass spectra of the cluster during synthesis. The black traces represent the MALDI MS spectra, and the red traces represent the LDI MS spectra. The corresponding UV/Vis spectra are shown in the insets.

By using the same process, we have also synthesized several silver clusters of masses 8.0, 22.8, 29.2, and 34.4 kDa. The UV/Vis spectra and MALDI MS spectra of these as-synthesized clusters are shown in Figure S16. We have assigned those peaks as $Ag_{\approx 38}L_{\approx 24}$, $Ag_{\approx 130}L_{\approx 52}$, $Ag_{\approx 170}L_{\approx 64}$, and $Ag_{\approx 202}L_{\approx 70}$ (L is *p*-*tert*-butylbenzenethiol). The larger spectral width and poor resolution at larger mass numbers made the assignments imprecise. However, for gold clusters, especially $Au_{25}SBB_{18}$ synthesized by this method, the spectrum was well-defined (Figure S17). It may be noted that silver cluster peaks are inherently broader as it has two stable isotopes (107 and 109), whereas gold has only one natural isotope (197).

Conclusions

We have developed a new strategy for the synthesis of a diverse array of clusters without a PTR, which is a persistent impurity for the previously reported two-phase methods. This process will help to create a series of monodisperse organic-soluble metal clusters. In particular, we have characterized a new cluster, $Ag_{68}SBB_{34}$, by using different analytical tools. The product is crystalline. We expect that the proposed synthetic strategy and the cluster synthesized will help to extend the area of atomically precise clusters.

Experimental Section

Only the synthesis and characterization of Ag_{68} are discussed here. More details are provided in the Supporting Information. Silver nitrate (20 mg) was dissolved in methanol (3 mL). To that solution, toluene (3 mL) was added, and the solution was constantly stirred.

 © 0000 Wiley-VCH Verlag GmbH & Co. KGaA, Weinheim

BBSH (ca. 132 μL) was then added. The solution changed from yellow to turbid yellow-white owing to the formation of $Ag^{I}SBB$ thiolates. After 30 min of stirring, ice cold water (2 mL) containing sodium borohydride (45 mg) was added to the solution with stirring. The solution changed to dark brown. Upon standing for 10 min, two distinct phases separated. The top phase contained the cluster in toluene. The toluene solution was used for the measurement of the time-dependent UV/Vis and MALDI MS spectra. The time-dependent study showed that the reaction was complete within 120 min. After 120 min, the toluene phase containing the cluster was separated and dried by rotary evaporation. Then, the dried material was washed four to five times with methanol to remove excess thiol and other impurities. HPLC of this cleaned sample was performed with THF/MeOH (70:30) as the mobile phase. This confirmed the presence of a single cluster. From the MALDI and LDI MS study, we assigned the material as $Ag_{68}SBB_{38}$. The composition was further confirmed by thermogravimetric (TG) and EDAX analyses.

Chemicals: Silver nitrate ($AgNO_3$, AR grade) was purchased from RANKEM, India. Methanol (AR grade), toluene (AR grade), and chloroform (AR grade) were purchased from R. K. Scientific, India. 4-*tert*-Butylbenzenethiol (97%), 4-*tert*-butylbenzyl mercaptan, *trans*-2-[3-(4-tertbutylphenyl)-2-methyl-2-propenylidene]malononitrile (DCTB, 98%) matrix, and sodium borohydride ($NaBH_4$, 95%) were purchased from Sigma–Aldrich.

Instrumentation: Details are provided in the Supporting Information.

Supporting Information (see footnote on the first page of this article): MALDI MS, LDI MS, UV/Vis, and EDAX spectra; TEM images; SEM images; TGA curve; and XRD pattern.

Acknowledgments

The authors thank the Department of Science and Technology (DST), Government of India, New Delhi for constantly supporting our research program on nanomaterials. A. G. thanks the Council of Scientific and Industrial Research (CSIR), New Delhi for a fellowship.

[1] a) R. L. Whetten, J. T. Khoury, M. M. Alvarez, S. Murthy, I. Vezmar, Z. L. Wang, P. W. Stephens, C. L. Cleveland, W. D. Luedtke, U. Landman, *Adv. Mater.* **1996**, *8*, 428–433; b) A. Desireddy, B. E. Conn, J. Guo, B. Yoon, R. N. Barnett, B. M. Monahan, K. Kirschbaum, W. P. Griffith, R. L. Whetten, U. Landman, T. P. Bigioni, *Nature (London, U. K.)* **2013**, *501*, 399–402; c) H. Yang, Y. Wang, H. Huang, L. Gell, L. Lehtovaara, S. Malola, H. Häkkinen, N. Zheng, *Nat. Commun.* **2013**, *4*, 2422; d) H. Häkkinen, *Nat. Chem.* **2012**, *4*, 443–455; e) T. Udayabhaskararao, Y. Sun, N. Goswami, S. K. Pal, K. Balasubramanian, T. Pradeep, *Angew. Chem. Int. Ed.* **2012**, *51*, 2155–2159; *Angew. Chem.* **2012**, *124*, 2197; f) C. Zeng, H. Qian, T. Li, G. Li, N. L. Rosi, B. Yoon, R. N. Barnett, R. L. Whetten, U. Landman, R. Jin, *Angew. Chem. Int. Ed.* **2012**, *51*, 13114–13118; *Angew. Chem.* **2012**, *124*, 13291; g) J. Koivisto, S. Malola, C. Kumara, A. Dass, H. Häkkinen, M. Pettersson, *J. Phys. Chem. Lett.* **2012**, *3*, 3076–3080; h) O. M. Bakr, V. Amendola, C. M. Aikens, W. Wenseleers, R. Li, L. Dal Negro, G. C. Schatz, F. Stellacci, *Angew. Chem. Int. Ed.* **2009**, *48*, 5921–5926; *Angew. Chem.* **2009**, *121*, 6035–6040; i) I. Díez, M. Pusa, S. Kulmala, H. Jiang, A. Walther, A. S. Goldmann, A. H. E. Müller, O. Ikkala, R. H. A. Ras, *Angew. Chem. Int. Ed.* **2009**, *48*, 2122–2125; *Angew. Chem.* **2009**, *121*, 2156; j) H. Yao, M. Saeki, K. Kimura, *J. Phys. Chem. C* **2010**, *114*, 15909–15915; k) N. Nishida, H. Yao, K. Kimura, *Langmuir* **2008**, *24*, 2759–2766; l) N. Nishida, H. Yao, T. Ueda, A. Sasaki, K. Kimura, *Chem. Mater.* **2007**, *19*, 2831–2841; m) S. Knoppe, I. Dolamic, A. Dass, T. Bürgi, *Angew. Chem. Int. Ed.* **2012**, *51*, 7589–7591; *Angew. Chem.* **2012**, *124*, 7709; n) M. Walter, J. Akola, O. Lopez-Acevedo, P. D. Jadzinsky, G. Calero, C. J. Ackerson, R. L. Whetten, H. Gronbeck, H. Häkkinen, *Proc. Natl. Acad. Sci. USA* **2008**, *105*, 9157–9162; o) R. B. Wyrwas, M. M. Alvarez, J. T. Khoury, R. C. Price, T. G. Schaaff, R. L. Whetten, *Eur. Phys. J. D* **2007**, *43*, 91–95.

[2] a) M. Arenz, U. Landman, U. Heiz, *ChemPhysChem* **2006**, *7*, 1871–1879; b) Y. Liu, H. Tsunoyama, T. Akita, T. Tsukuda, *Chem. Commun.* **2010**, *46*, 550–552; c) A. Leelavathi, R. T. U. Bhaskara, T. Pradeep, *Nanoscale Res. Lett.* **2011**, *6*, 123; d) Y. Zhu, H. Qian, B. A. Drake, R. Jin, *Angew. Chem. Int. Ed.* **2010**, *49*, 1295–1298; *Angew. Chem.* **2010**, *122*, 1317; e) N. de Silva, J.-M. Ha, A. Solovyov, M. M. Nigra, I. Ogino, S. W. Yeh, K. A. Durkin, A. Katz, *Nat. Chem.* **2010**, *2*, 1062–1068.

[3] a) L. Polavarapu, M. Manna, Q.-H. Xu, *Nanoscale* **2011**, *3*, 429–434; b) M. M. A. Habeeb, P. K. Verma, S. K. Pal, A. Retnakumari, M. Koyakutty, S. Nair, T. Pradeep, *Chem. Eur. J.* **2010**, *16*, 10103–10112; c) A. M. Gobin, M. H. Lee, N. J. Halas, W. D. James, R. A. Drezek, J. L. West, *Nano Lett.* **2007**, *7*, 1929–1934; d) P. C. Ray, S. A. Khan, A. K. Singh, D. Senapati, Z. Fan, *Chem. Soc. Rev.* **2012**, *41*, 3193–3209.

[4] S. Sivaramakrishnan, P.-J. Chia, Y.-C. Yeo, L.-L. Chua, P. K. H. Ho, *Nat. Mater.* **2007**, *6*, 149–155.

[5] a) M. Brust, M. Walker, D. Bethell, D. J. Schiffrin, R. Whyman, *J. Chem. Soc., Chem. Commun.* **1994**, 801–802; b) M. Zhu, E. Lanni, N. Garg, M. E. Bier, R. Jin, *J. Am. Chem. Soc.* **2008**, *130*, 1138–1139; c) O. Toikkanen, V. Ruiz, G. Rönnholm, N. Kalkkinen, P. Liljeroth, B. M. Quinn, *J. Am. Chem. Soc.* **2008**, *130*, 11049–11055; d) M. Zhu, H. Qian, R. Jin, *J. Am. Chem. Soc.* **2009**, *131*, 7220–7221; e) M. Zhu, H. Qian, R. Jin, *J. Phys. Chem. Lett.* **2010**, *1*, 1003–1007; f) Y. Negishi, C. Sakamoto, T. Ohyama, T. Tsukuda, *J. Phys. Chem. Lett.* **2012**, *3*, 1624–1628.

[6] R. Mukhopadhyay, S. Mitra, M. Johnson, V. R. Rajeev Kumar, T. Pradeep, *Phys. Rev. B* **2007**, *75*, 075414.

[7] a) H. Qian, R. Jin, *Chem. Mater.* **2011**, *23*, 2209–2217; b) T. Udaya Bhaskara Rao, T. Pradeep, *Angew. Chem. Int. Ed.* **2010**, *49*, 3925–3929; *Angew. Chem.* **2010**, *122*, 4017.

[8] A. Ghosh, T. Udayabhaskararao, T. Pradeep, *J. Phys. Chem. Lett.* **2012**, *3*, 1997–2002.

[9] a) Y. Negishi, K. Nobusada, T. Tsukuda, *J. Am. Chem. Soc.* **2005**, *127*, 5261–5270; b) S. Kumar, M. D. Bolan, T. P. Bigioni, *J. Am. Chem. Soc.* **2010**, *132*, 13141–13143; c) N. Cathcart, V. Kitaev, *J. Phys. Chem. C* **2010**, *114*, 16010–16017.

[10] a) H. Qian, Y. Zhu, R. Jin, *J. Am. Chem. Soc.* **2010**, *132*, 4583–4585; b) H. Qian, M. Zhu, U. N. Andersen, R. Jin, *J. Phys. Chem. A* **2009**, *113*, 4281–4284; c) I. Chakraborty, A. Govindarajan, J. Erusappan, A. Ghosh, T. Pradeep, B. Yoon, R. L. Whetten, U. Landman, *Nano Lett.* **2012**, *12*, 5861–5866; d) Y. Negishi, R. Arai, Y. Niihori, T. Tsukuda, *Chem. Commun.* **2011**, *47*, 5693–5695; e) Z. Wu, M. A. MacDonald, J. Chen, P. Zhang, R. Jin, *J. Am. Chem. Soc.* **2011**, *133*, 9670–9673.

[11] A. Dass, *J. Am. Chem. Soc.* **2008**, *130*, 5940–5946.

[12] P. Ramasamy, S. Guha, E. S. Shibu, T. S. Sreeprasad, S. Bag, A. Banerjee, T. Pradeep, *J. Mater. Chem.* **2009**, *19*, 8456–8462.

[13] a) H. Qian, Y. Zhu, R. Jin, *ACS Nano* **2009**, *3*, 3795–3803; b) Y. Negishi, K. Igarashi, K. Munakata, W. Ohgake, K. Nobusada, *Chem. Commun.* **2012**, *48*, 660–662.

[14] E. Sumesh, M. S. Bootharaju, Anshup, T. Pradeep, *J. Hazard. Mater.* **2011**, *189*, 450–457.

[15] T. U. B. Rao, B. Nataraju, T. Pradeep, *J. Am. Chem. Soc.* **2010**, *132*, 16304–16307.

[16] H. Qian, R. Jin, *Nano Lett.* **2009**, *9*, 4083–4087.

Received: June 24, 2014
Published Online: ■

 © 0000 Wiley-VCH Verlag GmbH & Co. KGaA, Weinheim

EurJIC European Journal of Inorganic Chemistry

Silver Clusters

A. Ghosh, T. Pradeep* **1–7**

Synthesis of Atomically Precise Silver Clusters by Using the Miscibility Principle

Keywords: Cluster compounds / Phase diagrams / Silver / S ligands / Solvent effects

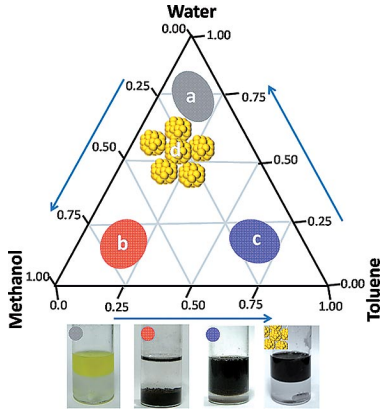

Silver and gold clusters have been synthesized by using the miscibility principle of solvents. Three solvents, that is, water, methanol, and toluene (or chloroform) have been used to synthesize different silver clusters by this method without phase-transfer agents. Separate regions of the phase diagram (a, b, c, and d) produce distinctly different clusters from the same reactant compositions.

 © 0000 Wiley-VCH Verlag GmbH & Co. KGaA, Weinheim